BIOCHEMISTRY
including biophysical chemistry & molecular biology
Article

Biochemistry **2009,** *48,* 6095–6103 6095
DOI: 10.1021/bi900317a

Effect of a Single-Amino Acid Substitution of the 43 kDa Chlorophyll Protein on the Oxygen-Evolving Reaction of the Cyanobacterium *Synechocystis* sp. PCC 6803: Analysis of the Glu354Gln Mutation[†]

Yuichiro Shimada,[‡] Hiroyuki Suzuki,[§] Tohru Tsuchiya,[‡] Tatsuya Tomo,[‡] Takumi Noguchi,[§] and Mamoru Mimuro*[,‡]

[‡]*Graduate School of Human and Environmental Studies, Kyoto University, Kyoto 606-8501, Japan, and* [§]*Institute of Materials Science, University of Tsukuba, Tsukuba, Ibaraki 305-8573, Japan*

Received February 24, 2009; Revised Manuscript Received May 23, 2009

ABSTRACT: We constructed a mutant (CP43-Glu354Gln) of the cyanobacterium *Synechocystis* sp. PCC 6803 in which the glutamic acid at position 354 of the 43 kDa chlorophyll protein (CP43) was replaced with glutamine. To determine the effect of this mutation on the reaction processes of the Mn cluster in the oxygen-evolving complex, we mainly analyzed the spectroscopic properties, including Fourier transform infrared (FTIR) spectroscopy, of photosystem II core complexes. Mutant cells exhibited a lower oxygen-evolving activity than wild-type cells, and an altered pattern of flash-dependent delayed luminescence. This phenotype differed somewhat from an earlier report of the same mutant [Strickler, M. A., et al. (2008) *Philos. Trans. R. Soc. London, Ser. B 363*, 1179−1187]. FTIR difference spectroscopy revealed that CP43-Glu354 functions as a ligand to the Mn cluster, most likely with bridging bidentate coordination to two Mn ions in the S_1 state and chelating bidentate coordination to a single Mn ion in the S_2 state. A single water molecule was bound to the same Mn atom to which CP43-Glu354 was ligated, and this Mn atom was oxidized in the S_1-to-S_2 transition. This is the first report on a binding site of a water molecule relevant to a specific amino acid ligand. We found that the Mn ion or ligand that is oxidized in the S_2-to-S_3 transition was not directly coupled to CP43-Glu354. While the definitive assignment of ligation to the Mn atoms is still under debate, our identification of a novel water binding site will lead to new insights into the oxygen evolution mechanism.

Photosynthesis sustains almost all organisms on the earth through primary production. During photosynthesis, the reduction of carbon dioxide to carbohydrate occurs through a reductive reaction that requires electrons. In oxygenic photosynthetic organisms, electrons are supplied by the cleavage of water molecules in a process termed photosynthetic oxygen evolution. Thus, the sustainability of human beings and nearly all other life forms is critically dependent on photosynthetic oxygen evolution.

The reaction processes underlying oxygen evolution have been studied extensively using many different approaches (*1*−*6*), including electron paramagnetic resonance (EPR) spectroscopy (*5*, *7*), X-ray absorption spectroscopy (*4*, *8*, *9*), Fourier transform infrared (FTIR)[1] spectroscopy (*6*, *10*), and X-ray crystallographic analysis (*11*−*15*). However, while crystallographic data of photosystem (PS) II complexes isolated from a few species of cyanobacteria have been reported (*11*−*15*), the reaction processes continue to be debated due to several ambiguities in structures, particularly that of the oxygen-evolving complex (OEC). The OEC consists of a cluster of four Mn atoms and a Ca^{2+} ion (*16*−*19*). At present, the mechanisms underlying ligation of amino acid moieties to the Mn cluster, the binding of water molecules to Mn atoms, the S-state transitions, and changes in valence state of the Mn atoms are unresolved.

Many model compounds of the Mn cluster have been synthesized (*20*, *21*); however, none of these compounds appear to accurately mimic the function of native OECs. An alternative approach is the construction of strains in which critical amino acids involved in ligation of the Mn cluster are mutated. Several such mutant strains have been generated, and a number of excellent review articles on the effect of these point mutations on the oxygen-evolving process have appeared (*22*−*24*). The mutants can be divided into two major categories: mutants of D1 protein (PsbA) and mutants of the 43 kDa chlorophyll (Chl) protein (CP43, PsbC). Several amino acids in the C-terminal region of D1 protein supply ligands to the Mn cluster and have been implicated in oxygen evolution. The alanine at position 344 of D1 protein (*25*−*30*), for example, is believed to be a ligand to

[†]This study was supported by a Grant-in-Aid for Creative Scientific Research (17GS0314) from the Japanese Society for the Promotion of Science (JSPS) to M.M. and T.N., by Grants-in-Aid for Scientific Research from the Ministry of Education, Culture, Sports, Science, and Technology, Japan (MEXT), to T. Tomo (19614007), and by a Grant-in-Aid for JSPS Fellows (19252) to H.S.

*To whom correspondence should be addressed: Graduate School of Human and Environmental Studies, Kyoto University, Kyoto 606-8501, Japan. Telephone: +81-75-753-6855. Fax: +81-75-753-6855. E-mail: mamo-mi@mm1.mbox.media.kyoto-u.ac.jp.

[1]Abbreviations: Chl, chlorophyll; CP, chlorophyll protein; DCMU, 3-(3,4)-dichlorophenyl-1,1-dimethylurea; DL, delayed luminescence; DM, *n*-dodecyl *β*-D-maltoside; FTIR, Fourier transform infrared; OEC, oxygen-evolving complex; PS, photosystem; TL, thermoluminescence; WT, wild type.

Published on Web 05/26/2009

Mn and/or Ca atoms in the Mn cluster. Similarly, crystallographic data indicate that CP43 also supplies a ligand to the Mn cluster (*13*−*15*). However, at present, the structural data are not sufficient for determining the role of CP43 in the reaction mechanisms of oxygen evolution.

In this work, we constructed a single amino acid substitution mutant of CP43 in which glutamic acid 354 was replaced with glutamine in the cyanobacterium *Synechocystis* sp. PCC 6803 (hereafter termed *Synechocystis*). Strickler et al. previously reported that the FTIR spectrum of CP43-Glu354Gln is dramatically different from that of wild-type (WT) CP43, which suggests that this residue is involved in ligation to the Mn cluster (*31*). To determine whether this mutation induced change(s) in the oxygen-evolving reaction, we analyzed CP43-Glu354Gln cells and PS II complexes using spectroscopic methods, including FTIR spectroscopy. We found strong evidence that CP43-Glu354 supplies a ligand to the Mn cluster and that a water molecule is bound to the same Mn atom to which CP43-Glu354 supplies a ligand. To the best of our knowledge, this is the first report of a water molecule coupled to a specific amino acid ligand in the Mn cluster. We discuss the implications of our results for ligation to Mn atoms and changes in valence state during the photosynthetic oxygen-evolving reactions.

EXPERIMENTAL PROCEDURES

Construction of the CP43-Glu354Gln Mutant. The CP43-Glu354Gln mutant strain was obtained by complementation of a CP43 deletion mutant strain with a mutated form of *psbC*. We obtained *Synechocystis* sp. PCC 6803 cells encoding a fusion protein of the 47 kDa chlorophyll protein (CP47, PsbB) and six His residues (*32*, *33*). A CP43 deletion mutant was obtained by replacement of the CP43 structural gene with a spectinomycin resistance cassette (*34*). We constructed a CP43 gene cassette, which contained *psbC* with its upstream and downstream regions and the kanamycin resistance gene, the last of which was inserted downstream of the *psbC* stop codon. A point mutation was introduced into *psbC* for codon Glu354 (GAA to CAA) to generate the mutant CP43 gene cassette. WT and CP43-Glu354Gln mutant cells were obtained by complementation of CP43 deletion mutants with WT and mutant CP43 gene cassettes, respectively. The *psbC* mutation in cells was confirmed by nucleotide sequencing using an ABI PRISM 3100 Genetic Analyzer. WT and mutant cells were grown under photomixotrophic conditions at 25 °C in BG11 medium containing 10 mM Tes buffer (pH 8.2) and 5 mM glucose. White light from a fluorescent lamp was provided continuously at an intensity of 30 μmol of photons m^{-2} s^{-1}, and air was continuously supplied through an air filter (Myrex, Millipore).

Isolation of PS II Complexes and Analysis of Subunit Composition. PS II complexes were isolated as previously described (*34*, *35*). Briefly, cells were suspended in a buffer [50 mM Mes-NaOH buffer (pH 6.0) containing 10 mM $MgCl_2$, 5 mM $CaCl_2$, and 25% glycerol] and broken using glass beads. Thylakoid membranes were recovered by preparative centrifugation (2000*g* for 5 min at 4 °C) followed by centrifugation (40000*g* for 20 min at 4 °C) and resuspended in the same buffer with a Chl concentration of 1 mg/mL. PS II complexes were solubilized from thylakoid membranes with 0.8% dodecyl β-D-maltoside (DM) for 20 min at 4 °C in the dark and then purified by Ni^{2+} affinity column chromatography (ProBond resin, Invitrogen). The purified PS II was concentrated and dissolved in the buffer [50 mM Mes-NaOH buffer (pH 6.0) containing 10 mM $MgCl_2$, 5 mM $CaCl_2$, 25% glycerol, and 0.04% DM]. The subunit composition of PS II complexes was analyzed by sodium dodecyl sulfate−polyacrylamide gel electrophoresis (SDS−PAGE), as previously described (*36*). The stacking gel and running gels contained 4.5 and 16−22% acrylamide, respectively. Proteins were visualized by Coomassie Brilliant Blue R-250 staining. Western blotting was performed as previously described (*34*, *35*). Antibody raised against PS I proteins (*37*) and HRP-conjugated anti-IgG were used.

Oxygen-Evolving Activity. Oxygen-evolving activity was measured using a Clark-type oxygen electrode (Rank Brothers). Light from a projector lamp (1000 W halogen lamp) was collected with convex lenses at the front of an electrode vessel, and the light intensity was adjusted using neutral density filters (Toshiba). The Chl content of the algal suspensions was maintained at approximately 2 μg/mL so that actinic light was able to reach the rear of the electrode vessel. For measurements of activity in PS II core complexes, samples were suspended in a 50 mM Mes-NaOH buffer (pH 6.5) containing 1 M sucrose, 25 mM $CaCl_2$, and 10 mM NaCl. An electron acceptor (4 mM potassium ferricyanide) was also added. The Chl content of the complexes was approximately 4 μg/mL; however, an actual Chl content of individual samples was determined using a combination of extraction with either methanol or 80% acetone, spectroscopy (Hitachi U-2010), and the extinction coefficient of Porra et al. (*38*).

Optical Measurements. Absorption and steady-state fluorescence spectra were measured using a Hitachi 557 spectrophotometer and a Hitachi 850 spectrofluorometer, respectively (*33*, *39*). To assess the low-temperature fluorescence spectrum, polyethylene glycol [i.e., PEG, average molecular weight of 3350, final concentration of 15% (w/v), Sigma-Aldrich] was added to yield a homogeneous ice. The spectral sensitivity of the fluorometer was corrected using a substandard lamp with a known radiation profile.

Thermoluminescence (TL) and delayed luminescence (DL) were measured using a laboratory-built apparatus, as described previously (*40*, *41*). For TL measurements, an aliquot (75 μL) of a thylakoid suspension (0.3 mg of Chl/mL) in a buffer [50 mM Mes-NaOH buffer (pH 6.0) containing 10 mM $MgCl_2$, 5 mM $CaCl_2$, and 25% glycerol] or a core suspension (0.2 mg of Chl/mL) in the same buffer with additional 0.04% DM was loaded onto a piece of filter paper (1.5 cm × 1.5 cm). For B bands ($S_2Q_B^-$ or $S_3Q_B^-$ recombination), the thylakoid membranes were illuminated by one or two (1 s interval) flashes from a Xe-flash source (SL-230S, Sugawara) at 5 °C after preillumination with continuous white light (1 mW cm^{-2}) for 30 s at 25 °C with subsequent dark incubation for 15 min at the same temperature, while for Q bands ($S_2Q_A^-$ recombination), the thylakoid membranes or PS II core suspension in the presence of 50 μM 3-(3,4)-dichlorophenyl-1,1-dimethylurea (DCMU) was illuminated with continuous white light (80 mW cm^{-2}) for 10 s at −20 °C. The illuminated samples were quickly frozen and then warmed at a rate of 40 °C/min to record TL glow curves. For DL measurements, a thylakoid suspension (50 μg of Chl/mL, 100 μL) in a hollow aluminum holder (15 mm in diameter, 0.5 mm in depth) was illuminated with a series of Xe flashes (0.5 Hz) at 20 °C, and the DL intensity 1.8 s after each flash was recorded. The DL measurements were repeated three times with 15 min intervals of dark adaptation at 25 °C, and the average was calculated as a final datum.

For FTIR measurements, PS II core complexes suspended in a 10 mM Mes-NaOH buffer (pH 6.0) containing 5 mM NaCl, 5 mM $CaCl_2$, and 0.06% DM were concentrated to approximately 4.5 mg of Chl/mL using a Microcon-100 filter (Amicon). For S_3/S_2 spectra, 40 mM sucrose was added to increase the transition efficiency. An aliquot of the sample suspension (5 μL) was mixed with 1 μL of 100 mM potassium ferricyanide and dried on a CaF_2 plate (25 mm in diameter) under N_2 gas in an oval shape (6 mm × 9 mm). The sample was moderately hydrated or deuterated by placing 2 μL of a 40% (v/v) glycerol/H_2O or glycerol$(OD)_3$ (CDN, 98.7 at. % D)/D_2O (CDN, 99.9 at. % D) solution, respectively, in a sealed IR cell without touching the sample (*42*, *43*). The sample temperature was maintained at 10 °C by a circulating cold water bath in a copper holder. Flash-induced FTIR difference spectra were recorded using a Bruker IFS-66/S spectrophotometer and a Q-switched Nd:YAG laser (Quanta-Ray GCR-130; 532 nm; ~7 ns full width at half-maximum) (*42*, *43*). For S_2/S_1 measurements, samples were adapted to the dark for 20 min, and then single-beam spectra (50 s accumulation) were recorded before and after a single saturating flash. The measurement cycle was repeated 54 and 72 times for hydrated WT and CP43-Glu354Gln samples, respectively, and 40 and 36 times for deuterated WT and CP43-Glu354Gln samples, respectively. For S_3/S_2 measurements, samples were adapted to the dark for 20 min and then subjected to two flashes at an interval of 10 s. Spectra were recorded before, between, and after the flashes. The difference spectrum after the second flash was taken as the S_3/S_2 difference. This cycle was repeated 16 and 51 times for WT and mutant samples, respectively. All spectra were recorded at a resolution of 4 cm^{-1}.

RESULTS

Absorption and Fluorescence Spectra. CP43-Glu354Gln mutants grew at a slightly slower rate than WT cells. The doubling time for WT cells was 16 h, while that of mutant cells was 21 h. Figure 1 (inset) shows the absorption spectra of WT and mutant cells at 25 °C. When normalized to the Q_y band of Chl *a*, the two spectra were similar, with the exception of a small difference in the carotenoid region. The absorption spectra of the Q_y and Soret regions of Chl *a* were identical, and the absorption of phycobilin, mainly phycocyanin, was similar.

Fluorescence spectra were recorded at −196 °C and are shown in Figure 1. When Chl *a* of WT and mutant cells was preferentially excited at 435 nm, three bands were observed at 686, 695, and 724 nm (Figure 1a), corresponding to PS II, PS II, and PS I Chl *a*, respectively. The spectra of WT (black line) and mutant (red line) cells in the region of PS I Chl *a* fluorescence were superimposable, whereas the intensity of the PS II Chl *a* bands in mutant cells was increased by 15% over that of WT; however, the peak wavelength was the same. These results suggested that the PS II content per unit amount of Chl *a* is slightly higher in mutant cells. When phycocyanin was preferentially excited at 600 nm (Figure 1b), there was a significant difference in the PS I Chl *a* region between WT (black line) and mutant (red line) cells. When the spectra were normalized at 686 nm, the peak intensity at 724 nm of the mutant was 30% lower than that of WT cells. These results indicated that there is a low efficiency of energy transfer from phycocyanin to PS I Chl *a* in mutant cells. When the two spectra were normalized at 665 nm, which corresponds to allophycocyanin, mutant cells exhibited slightly higher peak intensities at 686 and 695 nm (data not shown), which indicated

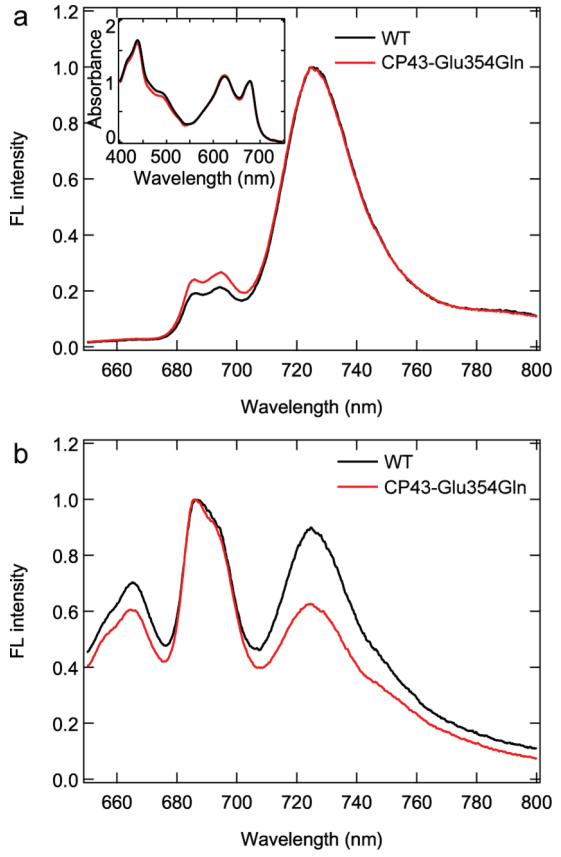

FIGURE 1: Fluorescence spectra of WT and CP43-Glu354Gln *Synechocystis*. Spectra were recorded at −196 °C at excitation wavelengths of 435 (a) and 600 nm (b). The spectra were normalized at the 724 nm peak of PS I Chl *a* (a) or at the 686 nm peak of PS II Chl *a* (b): WT, black lines; CP43-Glu354Gln mutant, red lines. The inset shows the absorption spectra of WT and CP43-Glu354Gln cells measured at room temperature.

a higher efficiency of energy transfer to PS II Chl *a*, but a lower efficiency of energy transfer to PS I Chl *a*. Thus, in CP43-Glu354Gln mutants, an energy transfer efficiency from phycocyanin or allophycocyanin to Chl *a* in thylakoid membranes appeared to be altered.

Polypeptide Composition of PS II Complexes. Figure 2 shows the polypeptide composition of thylakoid membranes and purified PS II core complexes from WT and CP43-Glu354Gln mutant cells. It was difficult to identify individual PS II subunits in thylakoid membranes because the levels of PS I (~60 kDa), phycobiliproteins (~16 kDa), and a few other membrane proteins were high in both samples. These protein bands were drastically reduced in intensity in preparations of purified PS II complexes, and the major PS II polypeptide bands were clearly found. The five major bands in the 30−50 kDa region corresponded to CP47, CP43, D1, D2, and the manganese-stabilizing protein PsbO. In the low-molecular mass region of the gel (< 20 kDa), the extrinsic proteins of the OEC (PsbU and PsbV) and the large subunit of cyt b_{559} (PsbE) were evident. There were no significant differences in protein composition between WT and CP43-Glu354Gln complexes based on SDS−PAGE analysis. These patterns were essentially similar to those of other PS II complexes so far isolated using a His tag (*28*, *45*). Contamination of PS I complexes was checked by Western blotting using the anti-PS I antibody and estimated to be less than a limit of detection [< 5% of that in thylakoid membranes (data not shown)]. Spectroscopic analysis gave more reliable results; the P700 contamination was < 1% on

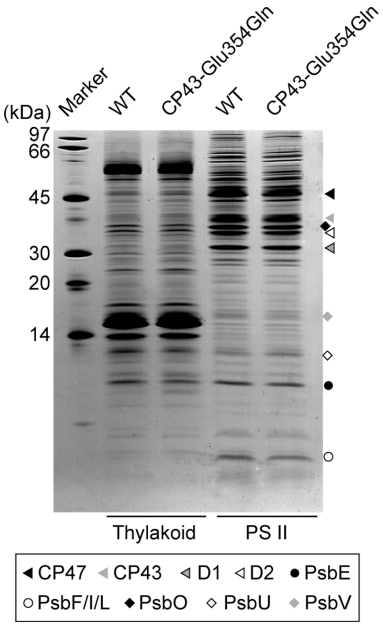

FIGURE 2: SDS−PAGE of thylakoid membranes and purified PS II complexes from WT and CP43-Glu354Gln *Synechocystis*. The amount of protein corresponding to 1 μg of Chl *a* was loaded in each lane. Polypeptides with molecular masses lower than that of PsbE were assigned on the basis of the previous report by Kashino et al. (*44*).

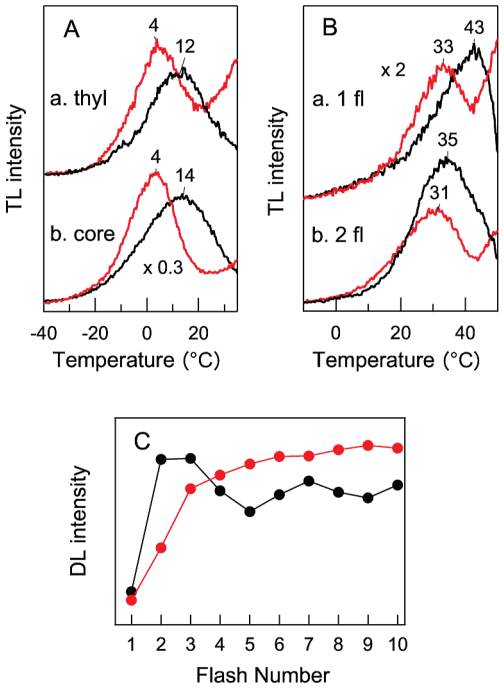

FIGURE 3: Thermoluminescence (TL) and flash-number dependence of delayed luminescence (DL) of WT and CP43-Glu354Gln *Synechocystis*. (A) TL glow curves of thylakoid membranes (a) and core complexes (b) from WT (black lines) and CP43-Glu354Gln (red lines) cells in the presence of DCMU. Illumination was performed at −20 °C with continuous white light. (B) TL glow curves of thylakoid membranes from WT (black lines) and CP43-Glu354Gln (red lines) cells after illumination via one flash (a) and two flashes (b) in the absence of DCMU. The flash illumination was performed at 5 °C. (C) Flash-number dependence of DL of thylakoid membranes from WT (black circles) and CP43-Glu354Gln (red circles) cells induced by successive flashes (0.5 Hz). Measurements were performed at 20 °C, and the DL intensity 1.8 s after each flash was monitored.

the Chl *a* basis (data not shown). These results indicated that OEC-containing PS II core complexes could be successfully purified from both types of cells.

Oxygen-Evolving Activity. The oxygen-evolving activity of WT cells was 354 ± 18 μmol of O_2 (mg of Chl)$^{-1}$ h^{-1}, while that of CP43-Glu354Gln mutant cells was 77 ± 8 μmol of O_2 (mg of Chl)$^{-1}$ h^{-1} under the saturating light intensity. On the other hand, the oxygen-evolving activity of isolated PS II complexes was 1960 ± 77 and 424 ± 12 μmol of O_2 (mg of Chl)$^{-1}$ h^{-1} for WT and mutant complexes, respectively. These activities ensured enrichment of PS II in our preparations.

TL and DL Analysis. We then measured TL and DL of cells. TL is an outburst of light emission occurring at a characteristic temperature when preilluminated and subsequently frozen organisms are warmed gradually in the darkness. This is known to arise from reversal of light-driven charge separation in PS II through a thermally activated recombination between the positive charge accumulated in the intermediate of water oxidation system on its donor side and the negative charge stabilized on the primary or secondary quinone acceptor on its acceptor side. This gives us information about both sides of PS II (*46*).

Figure 3A shows the TL glow curves of thylakoid membranes (a) and core complexes (b) from WT (black lines) and the CP43-Glu354Gln mutant (red lines) in the presence of DCMU. In both preparations, the so-called Q-band arising from $S_2Q_A^-$ recombination was observed at 12−14 °C in WT and at 4 °C, a temperature lower by 8−10 °C in CP43-Glu354Gln. The glow curves of the core complexes very similar to those of thylakoid membranes indicate that the Mn cluster retained its native structure during preparation of the core complexes.

Upon single-flash illumination on the WT thylakoid membranes in the absence of DCMU, the B_2 band arising from the $S_2Q_B^-$ state was observed at 43 °C (Figure 3Ba, black line). The corresponding TL peak of the CP43-Glu354Gln mutant was detected at 33 °C (red line), a temperature lower by 10 °C. This downshift of the B_2 band was in good agreement with that of the Q-band, reflecting a relatively large upshift in the S_2/S_1 redox potential by mutation. The presence of the Q and B_2 band in the CP43-Glu354Gln mutant with intensities comparable to that of WT indicates that the Mn cluster was fully assembled and the S_1-to-S_2 transition efficiently took place in this mutant.

Upon two flashes, the B_1 band due to $S_3Q_B^-$ recombination was detected at 35 and 31 °C in the WT and CP43-Glu354Gln thylakoid membranes, respectively (Figure 3Bb). The temperature decrease of the B_1 band by 4 °C by mutation was smaller than the value of ~10 °C in the B_2 band. Thus, the redox potential of the S_3/S_2 redox couple was only slightly upshifted by this mutation in contrast to the S_2/S_1 couple. The presence of the B_1 band in CP43-Glu354Gln, although the intensity was slightly lower than that of WT (Figure 3Bb), indicates that the S_2-to-S_3 transition was also active in this mutant. This idea was fully supported by the second-flash FTIR difference spectrum of this mutant providing S_3/S_2 signals similar to those of WT (see below).

DL arises from charge recombination between a positive charge on the donor side in PS II and a negative charge on the acceptor side in PS II and is monitored in real time without freezing. This is suitable for successive measurements on the redox state of PS II. The flash-number dependence of the DL signals originating from $S_2Q_B^-$ or $S_3Q_B^-$ recombination is shown in Figure 3C. The WT thylakoid membranes exhibited a clear oscillation pattern (black circle), although the period four

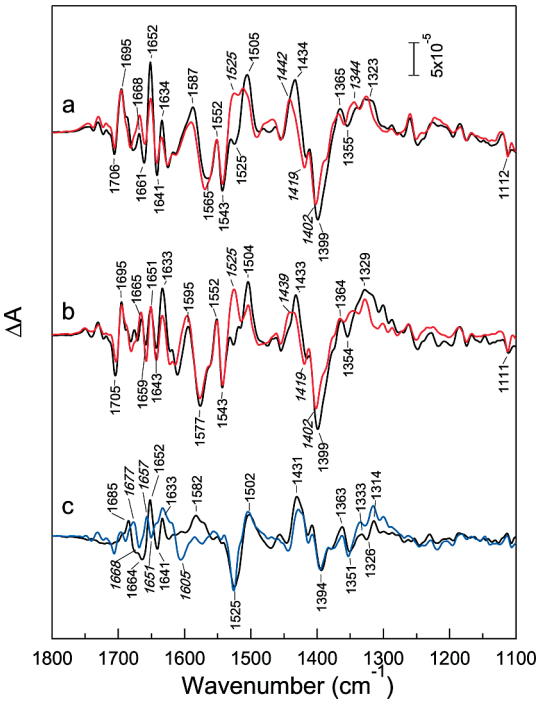

FIGURE 4: S_2/S_1 FTIR difference spectra in the 1800−1100 cm^{-1} region of PS II core complexes from *Synechocystis*. Hydrated (a) and deuterated (b) PS II core complexes: WT, black lines; CP43-Glu354Gln mutant, red lines. (c) WT-minus-Glu354Gln double difference spectra in H_2O (black line) and D_2O (blue line).

oscillation was slightly retarded after the second cycle probably due to the relatively long flash interval (2 s) and 25% population of the S_0 state as an initial state. In contrast, in CP43-Glu354Gln thylakoid membranes, there was an initial increase in DL intensity with the first three flashes, but the intensity became rather flat with only a gradual increase after the third flash (red circle). It is most likely that the S_2-to-S_3 transition is less effective in the mutant and the transition after the S_3 state is significantly retarded. The less effective S_2-to-S_3 transition is consistent with the lower TL intensity of the B_1 band versus that of WT (Figure 3Bb) and also the flash-induced FTIR data (see below).

FTIR Spectroscopy. Figure 4a shows the S_2/S_1 difference spectra of hydrated films of PS II core complexes from WT (black line) and CP43-Glu354Gln mutant (red line) cells. The asymmetric and symmetric carboxylate stretching regions of the mutant spectrum (1600−1500 and 1450−1300 cm^{-1}, respectively) were dramatically altered as compared to those of WT. In particular, the 1505 cm^{-1} peak was weakened, and a positive band appeared at 1525 cm^{-1}. The intensities of the positive and negative bands at 1434 and 1399 cm^{-1} were decreased and shifted to 1442 and 1402 cm^{-1}, respectively. Smaller frequency shifts and changes in intensity were also observed in the 1587/1565 cm^{-1} bands and in 1365−1320 cm^{-1} regions. There were also intensity changes in the peaks at 1680−1630 cm^{-1} of the amide I region.

Similar changes were detected when deuterated samples were analyzed (Figure 4b). In the mutant spectrum, the magnitude of the 1504 cm^{-1} band decreased and a new band appeared at 1525 cm^{-1} as compared to WT, while the bands at 1433/1399 cm^{-1} shifted to 1439/1402 cm^{-1} and were less intense. The changes in intensity in the 1595/1577 cm^{-1} bands were much smaller than those of corresponding bands at 1587/1565 cm^{-1} in the hydrated samples. Some small changes were also observed in the 1680−1630 and 1365−1320 cm^{-1} regions, similar to the hydrated samples.

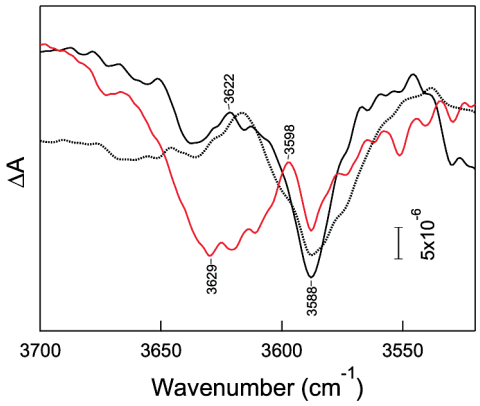

FIGURE 5: Weakly H-bonded OH stretching region of water in S_2/S_1 FTIR difference spectra of hydrated PS II core complexes from *Synechocystis*: WT, black solid line; CP43-Glu354Gln mutant, red solid lines. The S_2/S_1 spectrum of PS II core complexes from *T. elongatus* (*43*) is also shown for the sake of comparison (black dashed line).

The spectral differences between CP43-Glu354Gln and WT complexes were more evident in WT-minus-Glu354Gln double difference spectra (Figure 4c). In hydrated samples (black line), prominent bands were observed at 1525(−)/1502(+) and 1431(+)/1394(−) cm^{-1} in the asymmetric and symmetric carboxylate stretching regions, respectively. These bands were virtually insensitive to deuteration (blue line). In the asymmetric carboxylate stretching region, a positive band was observed at 1582 cm^{-1} in hydrated samples, which disappeared upon deuteration. Thus, this band probably does not involve carboxylate vibrations. The origin of this band is not clear at present, although it might involve the vibration of an exchangeable proton. Small peaks that were for the most part insensitive to deuteration were observed at 1363, 1351, 1333, 1326, and 1314 cm^{-1}. Among the complex features in the amide I region, peaks at 1685, 1664, 1652, 1641, and 1633 cm^{-1} were changed to peaks at 1677, 1668, 1657, 1651, 1633, and 1605 cm^{-1}, respectively, upon deuteration.

Figure 5 shows the weakly H-bonded OH region of the S_2/S_1 difference spectra of WT (black line) and CP43-Glu354Gln (red line) PS II complexes. The corresponding region of the spectrum of *Thermosynechococcus elongatus* (black dotted line) (*43*) is also shown for the sake of comparison. Despite some distortion of the baseline, positive and negative bands at 3622 and 3588 cm^{-1} were present in WT spectra, which corresponded to bands at 3617 and 3588 cm^{-1} in *T. elongatus*, respectively. These bands have been definitively assigned to the OH stretching vibration of an active water molecule coupled to the Mn cluster by $H_2{}^{18}O$ substitution (*42*, *43*). The spectral features of CP43-Glu354Gln complexes were significantly different from those of WT. A large, broad negative band at 3629 cm^{-1} and a relatively sharp positive peak at 3598 cm^{-1} were observed, while the positive band at approximately 3620 cm^{-1} disappeared. Although there appeared to be a negative peak at 3588 cm^{-1} in the mutant spectrum, the relative intensity was much smaller than that of WT. These results indicated that the water molecule interaction detected in the S_2/S_1 difference spectrum was drastically affected by substitution of Glu354 with Gln.

The S_3/S_2 difference spectra of hydrated films were measured by applying two flashes to the samples and calculating the difference spectra upon the second flash (Figure 6a). Note that

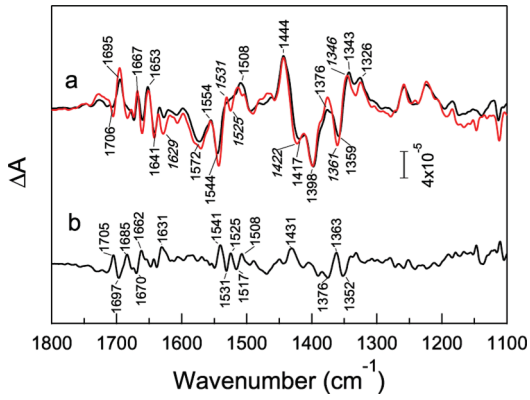

FIGURE 6: S_3/S_2 FTIR difference spectra in the 1800−1100 cm^{-1} region of PS II core complexes from *Synechocystis*. (a) Spectra of hydrated PS II complexes: WT, black line; CP43-Glu354Gln mutant, red line. The mutant spectrum was multiplied by 1.6 to adjust the intensity of the WT spectrum. The scale bar represents the intensity of the WT spectrum. (b) WT-minus-CP43-Glu354Gln double difference spectrum.

the first-flash spectra of the samples were virtually identical to the spectra shown in Figure 4. Although the intensities of the first-flash spectra were comparable between the WT and mutant, the intensity of the second-flash spectrum of the mutant was smaller by a factor of 1.6 than that of the WT spectrum (the mutant spectrum was scaled to compare with the WT spectrum in Figure 6a), being consistent with the lower efficiency of the S_2-to-S_3 transition observed in the TL and DL measurements (see above). The second-flash spectra of WT (Figure 6a, black line) and CP43-Glu354Gln mutant (Figure 6a, red line) complexes were very similar, with no prominent differences between them, indicating that the S_3/S_2 difference spectrum was correctly obtained in this mutant. Upon closer inspection, however, it was found that new small peaks at 1531 and 1525 cm^{-1} appeared in the mutant spectrum and the bands at 1450−1320 cm^{-1} in the symmetric carboxylate stretching region were slightly shifted. These minor differences were more evident in the WT-minus-Glu354Gln double difference spectrum (Figure 6b). Small peaks were observed in the regions of 1450−1320, 1550−1500, and 1700−1630 cm^{-1}. However, the intensities of these peaks were much smaller than those of the major peaks at 1525/1502 and 1431/1394 cm^{-1} in the double difference S_2/S_1 spectrum, but rather comparable to the minor peaks in this spectrum (Figure 4c).

It is worth noting that as additional flashes were applied to the CP43-Glu354Gln core complexes, we only detected small signals (with $\sim^1/_3$ of the intensity of the second-flash spectrum) virtually identical to those of the S_3/S_2 spectrum at the third flash, which most likely arose from a residual fraction by the miss of the second flash. The S_0/S_3 signals were not observed in contrast to WT core complexes, which generated typical S_0/S_3 and S_1/S_0 spectra at the third and fourth flashes, respectively (data not shown). These results indicated that the ability to transition from the S_3 state was rather inhibited in core complexes from the CP43-Glu354Gln mutant, consistent with the results of DL analysis (Figure 3C).

DISCUSSION

Significance of the CP43 Mutation. Previous studies have shown that site-directed mutagenesis of specific amino acids in D1 protein is a valuable tool for analyzing the structure and reaction processes of the OEC (*22*−*24*, *45*, *47*). Crystal structures of PS II complexes show that CP43 is also a component of and involved in OEC function (*13*−*15*), yet there have been few studies examining the effect of specific amino acid mutations of CP43 (*31*, *48*−*50*). A recent study by Strickler et al. (*31*) indicated that mutation of Glu354 of CP43 has a significant effect on the OEC. In the study presented here, we independently generated and analyzed a similar mutation of CP43. Our results differed somewhat from previously published data but suggest that, similar to D1 protein, mutational analysis of CP43 represents a promising tool for analyzing the OEC.

The phenotype of our CP43 mutant differed somewhat from previous reports (*31*). The oxygen-evolving activity of CP43-Glu354Gln cells was approximately 21% of that of WT under the light saturation conditions. In isolated PS II complexes, the activity of mutant complexes was approximately 21% of that of WT, which was consistent with previously published data (*31*). Even though an exceptionally high activity reported by Strickler et al. (*31*) was not reproduced in WT PS II complexes, an activity of our preparation was comparable to other reports (*51*, *52*). The oscillation pattern of the OEC in our mutant examined on thylakoid membranes by DL measurements differed significantly from that on thylakoid membranes by flash-oxygen yield in the previous study (*31*). The DL signal due to $S_2Q_B^-$ or $S_3Q_B^-$ recombination increased up to the third flash but was almost flat after that, and thus, no apparent oscillation was detected (Figure 3C). This observation was explained by a slightly lower efficiency of the S_2-to-S_3 transition and significantly retarded transitions beyond the S_3 state. Our data showed no evidence of the presence of heterogeneous centers, with a minor fraction having a normal S-state cycle, as suggested by Strickler et al. (*31*). The observed difference between mutants generated in different laboratories remains to be clarified, including a difference in the detection methods, i.e., oxygen evolution and DL.

FTIR Analysis. Comparison of the S_2/S_1 FTIR difference spectra of CP43-Glu354Gln and WT (Figure 4a) PS II complexes revealed drastic changes in the carboxylate stretching regions between the spectra. The most prominent bands in the WT-minus-Glu354Gln double difference spectrum (Figure 4c) were the negative bands at 1525 and 1394 cm^{-1} and the positive bands at 1502 and 1431 cm^{-1}, which are attributed to asymmetric (high-frequency bands) and symmetric (low-frequency bands) carboxylate stretching vibrations. These results were similar to those of Strickler et al. (*31*); the peaks at 1525, 1502, 1431, and 1394 cm^{-1} correspond to those at 1588, 1520, 1429, and 1378 cm^{-1}, respectively, although the origin of the relatively large frequency difference between 1394 and 1378 cm^{-1} is unknown at present. In contrast to Strickler et al. (*31*), however, who reported that the positive band at 1588 cm^{-1} was absent in the CP43-Glu354Gln spectrum, in the current study, the band at 1587 cm^{-1} was only slightly weakened and shifted slightly in the positive direction. Furthermore, the corresponding band at 1595 cm^{-1} in deuterated samples exhibited a much smaller change in intensity. As a result, the positive band at 1582 cm^{-1} in the double difference spectrum (Figure 4c, blue line) disappeared upon deuteration, which indicates that this band does not originate from a carboxylate stretching vibration. These results suggest that the stretching bands at 1525 and 1394 cm^{-1} correspond to Glu354 in the S_1 state, and the bands at 1502 and 1431 cm^{-1} correspond to Glu354 in the S_2 state. The presence of prominent Glu354 bands in the S_2/S_1 FTIR difference spectrum indicates that the structure of the Glu354 carboxylate group is significantly perturbed in the

S_1-to-S_2 transition, most likely due to ligation to the Mn ion that is oxidized in this transition.

The frequency differences between the asymmetric and symmetric bands described above were 131 and 71 cm^{-1} for the carboxylate bands in the S_1 and S_2 states, respectively. Generally, the asymmetric−symmetric frequency difference ($\Delta\nu$) correlates with the coordination structure of a carboxylate ligand as follows (*53*, *54*): (i) in unidentate coordination, $\Delta\nu$ is much greater (greater than ~200 cm^{-1}) than the ionic value (~160 cm^{-1}); (ii) in chelating bidentate coordination, $\Delta\nu$ (less than ~100 cm^{-1}) is significantly lower than the ionic value; and (iii) $\Delta\nu$ of a bridging bidentate structure is close to the ionic value (~160 cm^{-1}). On the basis of these criteria, our results indicate that Glu354 is involved in bridging bidentate coordination in the S_1 state, which shifts to chelating bidentate coordination in the S_2 state. The observation that the asymmetric and symmetric Glu354 bands were insensitive to deuteration (Figure 4c, blue line) indicates that the carboxylate group of Glu354 does not interact with exchangeable protons.

The water OH region of the mutant PS II spectrum was also drastically changed relative to that of WT (Figure 5). Weakly H-bonded OH bands of an active water molecule at 3622(+)/3588(−) cm^{-1} were dramatically shifted to 3629(−)/3598(+) cm^{-1} in the mutant spectrum (Figure 5). This water molecule has been proposed to be a ligand to a Mn ion with an asymmetric hydrogen-bonded structure (*55*). The changes induced by the Glu354Gln mutation indicate that this amino acid substitution alters the interaction of this water molecule. Because Glu354 probably does not engage in hydrogen bonding (see above), the spectral changes in the water OH region are probably not due to a direct interaction of this water molecule with Glu354. More likely, this water molecule and Glu354 ligate the same Mn ion that is oxidized in the S_1-to-S_2 transition. Thus, perturbation of the electronic state of this Mn ion by substitution of Glu354Gln also affects its interaction with a water molecule. The possibility, however, that the interaction of the water molecule was perturbed through a hydrogen bond network and charge delocalization over the Mn cluster cannot be excluded.

There were only minor changes in the S_3/S_2 FTIR difference spectrum of CP43-Glu354Gln core complexes as compared to WT (Figure 6). The bands at 1502 and 1431 cm^{-1}, corresponding to Glu354 in the S_2 state (see above), were not observed as negative peaks in the WT-minus-Glu354Gln S_3/S_2 double difference spectrum (Figure 6b), which indicates that the Glu354 bands are not involved in the S_3/S_2 difference spectrum. Thus, Glu354 is not directly coupled to the Mn ion or ligand that is oxidized in the S_2-to-S_3 transition. The minor changes that were observed in the S_3/S_2 spectrum are likely due to the secondary effects of the CP43-Glu354Gln mutation on the carboxylate ligands of the Mn cluster and provide further evidence that the large changes that we observed in the S_2/S_1 difference spectrum arise from Glu354 itself directly interacting with the Mn ion that is oxidized in the S_1-to-S_2 transition.

Recent studies using quantum chemical calculations have suggested that the relationship between the frequency shifts of carboxylate vibrations and the Mn center being oxidized is not very simple, and a carboxylate group can exhibit a relatively large frequency shift even if it is not a direct ligand to the oxidized Mn (*56*, *57*). However, the interpretations of the FTIR data described above were further supported by the TL glow curves of WT and the CP43-Glu354Gln mutant. The peak temperatures of the Q and B_2 bands arising from $S_2Q_A^-$ and $S_2Q_B^-$ recombination, respectively, were lowered by 8−10 °C (Figure 3A,B), which indicates that the redox potential of the S_2/S_1 couple was significantly upshifted with the Glu354Gln mutation. In contrast, the change in the B_1 band due to $S_3Q_B^-$ recombination was much smaller (−4 °C) (Figure 3Bb), indicating a smaller upshift by mutation in the S_3/S_2 redox potential. These observations are consistent with the view that the Mn ion oxidized in the S_1-to-S_2 transition directly interacts with Glu354 and the center oxidized in the S_2-to-S_3 transition is not directly coupled to Glu354. Recent theoretical calculations on the Mn cluster model with proteinaceous ligands also predicted that CP43-Glu354 should provide an observable frequency shift upon oxidation of the coordinated Mn ion (*58*, *59*), supporting this view.

On the basis of our analysis of WT and mutant CP43 by FTIR spectroscopy (Figures 4−6), we have demonstrated the following: (i) CP43-Glu354 is a ligand to the Mn cluster, participating in bridging bidentate coordination in the S_1 state and chelating bidentate coordination in the S_2 state; (ii) one of the Mn ions that is ligated by CP43-Glu354 is oxidized in the S_1-to-S_2 transition; (iii) a water molecule, which has an asymmetric hydrogen bond structure, is bound to the same Mn ion that is ligated by CP43-Glu354 and is oxidized in the S_1-to-S_2 transition; and (iv) CP43-Glu354 does not directly interact with either the Mn ion or ligand that is oxidized in S_2-to-S_3 transition.

An Updated Model of the Mn Cluster Relevant to CP43-Glu354. On the basis of the crystal structure of PS II complexes from *T. elongatus* at 3.0 Å resolution, Loll et al. (*14*) proposed a model of the Mn cluster that involves several amino acid ligands: D1-Asp170, D1-Glu189, D1-His332, D1-Glu333, D1-Asp342, D1-Ala344, and CP43-Glu354Gln. Guskov et al. (*15*) recently published an improved structural model with 2.9 Å resolution that supported those ligand structures. Yano et al. (*60*, *61*) proposed a modified model based on extended X-ray absorption fine structure (EXAFS) data in which the coordination structure of the amino acid ligands is slightly different. In both models, CP43-Glu354 functions as a bridging ligand to two Mn ions in the larger Mn_3 component (Figure 7, Mn_B, Mn_C, and Mn_D) of the "3 + 1" structure of the Mn cluster. Our results are consistent with these previous models. Figure 7 shows a schematic structure of the Mn cluster in the S_1 state as modeled by Yano et al. (*61*), in which CP43-Glu354 ligates to both Mn_B and Mn_C. On the basis of our current findings, we propose an addition to the model in which a water molecule is coordinated to either Mn_B or Mn_C. With the transition to the S_2 state, the Mn that binds the water molecule is oxidized from Mn^{3+} to Mn^{4+}, and CP43-Glu354 becomes a chelating ligand to Mn_B or Mn_C. The Mn or ligand center that is oxidized in the S_2-to-S_3 transition is probably Mn_A, a dangling Mn that is somewhat separated from the Mn_3 cluster or its ligand. If a Mn atom or a ligand in the Mn_3 cluster were oxidized, Glu354 signals would appear in the S_3/S_2 FTIR difference spectrum due to charge delocalization or structural perturbation, which our data do not support (Figure 6).

Alanine 344 in the C-terminus of the D1 protein has been assigned as a unidentate ligand to a Mn atom, based on previous work in which the FTIR signals at ~1354 cm^{-1} in the S_1 state and ~1338 or ~1320 cm^{-1} in the S_2 state were downshifted when Ala was labeled with ^{13}C (*27*, *29*). Strickler et al. (*31*) recently suggested that the bands at 1351(−)/1334(+) cm^{-1} in the WT-minus-Glu354Gln double difference spectrum originate from Ala344. We also detected minor signals at 1351(−)/1333(+) cm^{-1} (Figure 4c). If Ala344 is coordinated to Mn_C, which is simultaneously ligated by Glu354, as in the model by

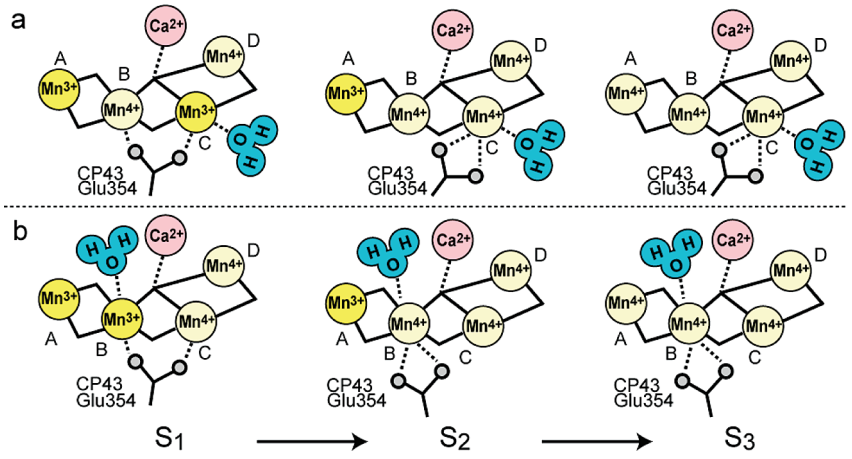

FIGURE 7: Schematic model of the ligation of CP43-Glu354 to the Mn cluster and binding of a water molecule. CP43-Glu354 is a ligand to the Mn cluster. It is involved in bridging bidentate coordination in the S_1 state and chelating bidentate coordination in the S_2 state. One of the Mn ions ligated by CP43-Glu354, Mn_C (a) or Mn_B (b), is oxidized in the S_1-to-S_2 transition. A water molecule is bound to the same Mn ion as CP43-Glu354, and this Mn ion is oxidized in the S_1-to-S_2 transition. CP43-Glu354 does not interact with the Mn ion or ligand that is oxidized in the S_2-to-S_3 transition.

Loll et al. (*14*), then oxidation of Mn_C in the S_1-to-S_2 transition (Figure 7a) is consistent with the presence of bands that correspond to both Glu354 and Ala344 in the S_2/S_1 difference spectrum. Alternatively, if Ala344 is coordinated to Mn_D, as modeled by Yano et al. (*61*), charge delocalization over the strongly coupled Mn_3 cluster or structural perturbation upon oxidation would affect the α-carboxylate vibration of D1-Ala344, which would be detected in the S_2/S_1 spectrum. Further studies are needed to resolve the structural details of CP43-Glu354 and D1-Ala344 in the PS II complex.

In summary, we have demonstrated that a water molecule is bound to the same Mn atom that is ligated by CP43-Glu354. Furthermore, we have shown that CP43-Glu354 is involved in different types of coordination, depending on the S state. CP43-Glu354 interacts with two Mn atoms in the S_1 state (Mn_B and Mn_C) and with only one of them in the S_2 state. While the assignment of ligation to Mn atoms is still under debate, our identification of a binding site of a water molecule will lead to new insights into the reaction processes and/or mechanism of the OEC. In this sense, the CP43-Glu354Gln mutant is a useful tool for further analysis.

ACKNOWLEDGMENT

We thank Prof. A. Tanaka (Hokkaido University, Sapporo, Japan) for providing an antibody raised against PsaA/B.

REFERENCES

(1) Kok, B., Forbush, B., and McGloin, M. (1970) Cooperation of charges in photosynthetic O_2 evolution. I. A linear four step mechanism. *Photochem. Photobiol. 11*, 457–475.
(2) Debus, R. J. (1992) The manganese and calcium ions of photosynthetic oxygen evolution. *Biochim. Biophys. Acta 1102*, 269–352.
(3) Hillier, W., and Wydrzynski, T. (2001) Oxygen ligand exchange at metal sites: Implications for the O_2 evolving mechanism of photosystem II. *Biochim. Biophys. Acta 1503*, 197–209.
(4) Sauer, K., and Yachandra, V. K. (2004) The water-oxidation complex in photosynthesis. *Biochim. Biophys. Acta 1655*, 140–148.
(5) Britt, R. D. (1996) Oxygen Evolution. In Oxygenic Photosynthesis: The Light Reactions (Ort, D. R., and Yocum, C. F., Eds.) pp 137−164, Kluwer Academic Publishers, Dordrecht, The Netherlands.
(6) Noguchi, T. (2008) Fourier transform infrared analysis of the photosynthetic oxygen-evolving center. *Coord. Chem. Rev. 252*, 336–346.
(7) Ahrling, K. A., Pace, R. J., and Evans, M. C. W. (2005) The Catalytic Manganese Cluster: Implication from Spectroscopy. In Photosystem II: The Light-Driven Water:Plastoquinone Oxidoreductase (Wydrzynski, T. J., and Satoh, K., Eds.) pp 285−306, Springer, Dordrecht, The Netherlands.
(8) Yachandra, V. K. (2002) Structure of the manganese complex in photosystem II: Insights from X-ray spectroscopy. *Philos. Trans. R. Soc. London, Ser. B 357*, 1347–1357.
(9) Yachandra, V. K. (2005) The Catalytic Manganese Cluster: Organization of the Metal Ions. In Photosystem II: The Light-Driven Water:Plastoquinone Oxidoreductase (Wydrzynski, T. J., and Satoh, K., Eds.) pp 235−260, Springer, Dordrecht, The Netherlands.
(10) Noguchi, T., and Berthomieu, C. (2005) Molecular Analysis by Vibrational Spectroscopy. In Photosystem II: The Light-Driven Water:Plastoquinone Oxidoreductase (Wydrzynski, T. J., and Satoh, K., Eds.) pp 367−387, Springer, Dordrecht, The Netherlands.
(11) Zouni, A., Witt, H. T., Kern, J., Fromme, P., Krauss, N., Saenger, W., and Orth, P. (2001) Crystal structure of photosystem II from *Synechococcus elongatus* at 3.8 Å resolution. *Nature 409*, 739–743.
(12) Kamiya, N., and Shen, J. R. (2003) Crystal structure of oxygen-evolving photosystem II from *Thermosynechococcus* vulcanus at 3.7-Å resolution. *Proc. Natl. Acad. Sci. U.S.A. 100*, 98–103.
(13) Ferreira, K. N., Iverson, T. M., Maghlaoui, K., Barber, J., and Iwata, S. (2004) Architecture of the photosynthetic oxygen-evolving center. *Science 303*, 1831–1838.
(14) Loll, B., Kern, J., Saenger, W., Zouni, A., and Biesiadka, J. (2005) Towards complete cofactor arrangement in the 3.0 Å resolution structure of photosystem II. *Nature 438*, 1040–1044.
(15) Guskov, A., Kern, J., Gabdulkhakov, A., Broser, M., Zouni, A., and Saenger, W. (2009) Cyanobacterial photosystem II at 2.9-Å resolution and the role of quinones, lipids, channels and chloride. *Nat. Struct. Mol. Biol. 16*, 334–342.
(16) Renger, G. (2007) Oxidative photosynthetic water splitting: Energetics, kinetics and mechanism. *Photosynth. Res. 92*, 407–425.
(17) Hillier, W., and Messinger, J. (2005) Mechanism of Photosynthetic Oxygen Production. In Photosystem II: The Light-Driven Water: Plastoquinone Oxidoreductase (Wydrzynski, T., and Satoh, K., Eds.) pp 567−608, Springer, Dordrecht, The Netherlands.
(18) McEvoy, J. P., and Brudvig, G. W. (2006) Water-splitting chemistry of photosystem II. *Chem. Rev. 106*, 4455–4483.
(19) Barber, J. (2008) Photosynthetic generation of oxygen. *Philos. Trans. R. Soc. London, Ser. B 363*, 2665–2674.
(20) Pecoraro, V. L., Baldwin, M. J., and Gelasco, A. (1994) Interaction of manganese with dioxygen and its reduced derivatives. *Chem. Rev. 94*, 807–826.
(21) Ruttinger, W., and Dismukes, G. C. (1997) Synthetic water-oxidation catalysts for artificial photosynthetic water oxidation. *Chem. Rev. 97*, 1–24.
(22) Debus, R. J. (2008) Protein Ligation of the Photosynthetic Oxygen-Evolving Center. *Coord. Chem. Rev. 252*, 244–258.
(23) Debus, R. J. (2001) Amino acid residues that modulate the properties of tyrosine Y(Z) and the manganese cluster in the water oxidizing complex of photosystem II. *Biochim. Biophys. Acta 1503*, 164–186.
(24) Diner, B. A. (2001) Amino acid residues involved in the coordination and assembly of the manganese cluster of photosystem II.

Proton-coupled electron transport of the redox-active tyrosines and its relationship to water oxidation. *Biochim. Biophys. Acta 1503*, 147–163.
(25) Nixon, P. J., Trost, J. T., and Diner, B. A. (1992) Role of the carboxy terminus of polypeptide D1 in the assembly of a functional water-oxidizing manganese cluster in photosystem II of the cyanobacterium *Synechocystis* sp. PCC 6803: Assembly requires a free carboxyl group at C-terminal position 344. *Biochemistry 31*, 10859–10871.
(26) Mizusawa, N., Kimura, Y., Ishii, A., Yamanari, T., Nakazawa, S., Teramoto, H., and Ono, T. (2004) Impact of replacement of D1 C-terminal alanine with glycine on structure and function of photosynthetic oxygen-evolving complex. *J. Biol. Chem. 279*, 29622–29627.
(27) Chu, H. A., Hillier, W., and Debus, R. J. (2004) Evidence that the C-terminus of the D1 polypeptide of photosystem II is ligated to the manganese ion that undergoes oxidation during the S1 to S2 transition: An isotope-edited FTIR study. *Biochemistry 43*, 3152–3166.
(28) Mizusawa, N., Yamanari, T., Kimura, Y., Ishii, A., Nakazawa, S., and Ono, T. (2004) Changes in the functional and structural properties of the Mn cluster induced by replacing the side group of the C-terminus of the D1 protein of photosystem II. *Biochemistry 43*, 14644–14652.
(29) Kimura, Y., Mizusawa, N., Yamanari, T., Ishii, A., and Ono, T. (2005) Structural changes of D1 C-terminal α-carboxylate during S-state cycling in photosynthetic oxygen evolution. *J. Biol. Chem. 280*, 2078–2083.
(30) Strickler, M. A., Walker, L. M., Hillier, W., and Debus, R. J. (2005) Evidence from biosynthetically incorporated strontium and FTIR difference spectroscopy that the C-terminus of the D1 polypeptide of photosystem II does not ligate calcium. *Biochemistry 44*, 8571–8577.
(31) Strickler, M. A., Hwang, H. J., Burnap, R. L., Yano, J., Walker, L. M., Service, R. J., Britt, R. D., Hillier, W., and Debus, R. J. (2008) Glutamate-354 of the CP43 polypeptide interacts with the oxygen-evolving Mn_4Ca cluster of photosystem II: A preliminary characterization of the Glu354Gln mutant. *Philos. Trans. R. Soc. London, Ser. B 363*, 1179–1187.
(32) Bricker, T. M., Morvant, J., Masri, N., Sutton, H. M., and Frankel, L. K. (1998) Isolation of a highly active photosystem II preparation from *Synechocystis* 6803 using a histidine-tagged mutant of CP 47. *Biochim. Biophys. Acta 1409*, 50–57.
(33) Mimuro, M., Akimoto, S., Tomo, T., Yokono, M., Miyashita, H., and Tsuchiya, T. (2007) Delayed fluorescence observed in the nanosecond time region at 77 K originates directly from the photosystem II reaction center. *Biochim. Biophys. Acta 1767*, 327–334.
(34) Shimada, Y., Tsuchiya, T., Akimoto, S., Tomo, T., Fukuya, M., Tanaka, K., and Mimuro, M. (2008) Spectral properties of the CP43-deletion mutant of *Synechocystis* sp. PCC 6803. *Photosynth. Res. 98*, 303–314.
(35) Tomo, T., Okubo, T., Akimoto, S., Yokono, M., Miyashita, H., Tsuchiya, T., Noguchi, T., and Mimuro, M. (2007) Identification of the special pair of photosystem II in a chlorophyll *d*-dominated cyanobacterium. *Proc. Natl. Acad. Sci. U.S.A. 104*, 7283–7288.
(36) Ikeuchi, M., and Inoue, Y. (1988) A new 4.8-kDa polypeptide intrinsic to the PS II reaction center, as revealed by modified SDS-PAGE with improved resolution of low-molecular-weight proteins. *Plant Cell Physiol. 29*, 1233–1239.
(37) Tanaka, A., Tanaka, Y., and Tsuji, H. (1994) Preferential accumulation of apoproteins of the light-harvesting chlorophyll *a*/*b*-protein complex in greening barley leaves treated with 5-aminolevulinic acid. *Planta 192*, 92–97.
(38) Porra, R. J., Thompson, W. A., and Kriedemann, P. E. (1989) Determination of accurate extinction coefficients and simultaneous equations for assaying chlorophylls *a* and *b* extracted with four different solvents: Verification of the concentration of chlorophyll standards by atomic absorption spectroscopy. *Biochim. Biophys. Acta 975*, 384–394.
(39) Mimuro, M., Akimoto, S., Yamazaki, I., Miyashita, H., and Miyachi, S. (1999) Fluorescence properties of chlorophyll *d*-dominating prokaryotic alga, *Acaryochloris marina*: Studies using time-resolved fluorescence spectroscopy on intact cells. *Biochim. Biophys. Acta 1412*, 37–46.
(40) Noguchi, T., Katoh, M., and Inoue, Y. (2002) A new system for detection of thermoluminescence and delayed luminescence from photosynthetic apparatus with precise temperature control. *Spectroscopy 16*, 89–94.
(41) Koyama, K., Suzuki, H., Noguchi, T., Akimoto, S., Tsuchiya, T., and Mimuro, M. (2008) Oxygen evolution in the thylakoid-lacking cyanobacterium *Gloeobacter violaceus* PCC 7421. *Biochim. Biophys. Acta 1777*, 369–378.
(42) Noguchi, T., and Sugiura, M. (2002) Flash-induced FTIR difference spectra of the water oxidizing complex in moderately hydrated photosystem II core films: Effect of hydration extent on S-state transitions. *Biochemistry 41*, 2322–2330.
(43) Noguchi, T., and Sugiura, M. (2002) FTIR detection of water reactions during the flash-induced S-state cycle of the photosynthetic water-oxidizing complex. *Biochemistry 41*, 15706–15712.
(44) Kashino, Y., Lauber, W. M., Carroll, J. A., Wang, Q., Whitmarsh, J., Satoh, K., and Pakrasi, H. B. (2002) Proteomic analysis of a highly active photosystem II preparation from the cyanobacterium *Synechocystis* sp. PCC 6803 reveals the presence of novel polypeptides. *Biochemistry 41*, 8004–8012.
(45) Chu, H. A., Nguyen, A. P., and Debus, R. J. (1995) Amino acid residues that influence the binding of manganese or calcium to photosystem II. 1. The lumenal interhelical domains of the D1 polypeptide. *Biochemistry 34*, 5839–5858.
(46) Inoue, Y (1996) Photosynthetic Thermoluminescence as Simple Probe of Photosystem II Electron Transport. In Biophysical Techniques in Photosynthesis (Amesz, J., and Hoff, A. J., Eds.) pp 93−107, Kluwer Academic Publishers, Dordrecht, The Netherlands.
(47) Chu, H. A., Nguyen, A. P., and Debus, R. J. (1995) Amino acid residues that influence the binding of manganese or calcium to photosystem II. 2. The carboxy-terminal domain of the D1 polypeptide. *Biochemistry 34*, 5859–5882.
(48) Rosenberg, C., Christian, J., Bricker, T. M., and Putnam-Evans, C. (1999) Site-directed mutagenesis of glutamate residues in the large extrinsic loop of the photosystem II protein CP 43 affects oxygen-evolving activity and PS II assembly. *Biochemistry 38*, 15994–16000.
(49) Knoepfle, N., Bricker, T. M., and Putnam-Evans, C. (1999) Site-directed mutagenesis of basic arginine residues 305 and 342 in the CP 43 protein of photosystem II affects oxygen-evolving activity in *Synechocystis* 6803. *Biochemistry 38*, 1582–1588.
(50) Hwang, H. J., Dilbeck, P., Debus, R. J., and Burnap, R. L. (2007) Mutation of arginine 357 of the CP43 protein of photosystem II severely impairs the catalytic S-state cycle of the H_2O oxidation complex. *Biochemistry 46*, 11987–11997.
(51) Kimura, Y., Mizusawa, N., Ishii, A., Nakazawa, S., and Ono, T. (2005) Changes in structural and functional properties of oxygen-evolving complex induced by replacement of D1-glutamate 189 with glutamine in photosystem II: Ligation of glutamate 189 carboxylate to the manganese cluster. *J. Biol. Chem. 280*, 37895–37900.
(52) Sakurai, I., Mizusawa, N., Wada, H., and Sato, N. (2007) Digalactosyldiacylglycerol is required for stabilization of the oxygen-evolving complex in photosystem II. *Plant Physiol. 145*, 1361–1370.
(53) Deacon, G. B., and Phillips, R. J. (1980) Relationships between the carbon-oxygen stretching frequencies of carboxylate complexes and the type of carboxylate coordination. *Coord. Chem. Rev. 33*, 227–250.
(54) Nakamoto, K. (1997) Infrared and Raman spectra of inorganic and coordination compounds , 5th ed., part B, pp 59−62, John Wiley & Sons, New York.
(55) Noguchi, T., and Sugiura, M. (2000) Structure of an active water molecule in the water-oxidizing complex of photosystem II as studied by FTIR spectroscopy. *Biochemistry 39*, 10943–10949.
(56) Siegbahn, P. E. M. (2008) Mechanism and energy diagram for O-O bond formation in the oxygen-evolving complex in photosystem II. *Philos. Trans. R. Soc. London, Ser. B 363*, 1221–1228.
(57) Gascón, J. A., Sproviero, E. M., McEvoy, J. P., Brudvig, G. W., and Batista, V. S. (2008) Ligation of the D-terminus of the D1 polypeptide of photosystem II to the oxygen evolving complex: A DFT-QM/MM study. In Photosynthesis. Energy from the Sun, 14th International Congress on Photosynthesis (Allen, J. F., Gantt, E., Golbeck, J. H., and Osmond, B., Eds.) pp 363−368, Springer, Dordrecht, The Netherlands.
(58) Sproviero, E. M., Gascón, J. A., McEvoy, J. P., Brudvig, G. W., and Batista, V. S. (2008) Quantum mechanics/molecular mechanics study of the catalytic cycle of water splitting in photosystem II. *J. Am. Chem. Soc. 130*, 3428–3442.
(59) Sproviero, E. M., McEvoy, J. P., Gascón, J. A., Brudvig, G. W., and Batista, V. S. (2008) Computational insights into the O_2-evolving complex of photosystem II. *Photosynth. Res. 97*, 91–114.
(60) Yano, J., Kern, J., Sauer, K., Latimer, M. J., Pushkar, Y., Biesiadka, J., Loll, B., Saenger, W., Messinger, J., Zouni, A., and Yachandra, V. K. (2006) Where water is oxidized to dioxygen: Structure of the photosynthetic Mn_4Ca cluster. *Science 314*, 821–825.
(61) Yano, J., and Yachandra, V. K. (2008) Where water is oxidized to dioxygen: Structure of the photosynthetic Mn_4Ca cluster from X-ray spectroscopy. *Inorg. Chem. 47*, 1711–1726.